Available online at www.sciencedirect.com

ScienceDirect

Energy Procedia 61 (2014) 2042 – 2045

Energy Procedia

The 6th International Conference on Applied Energy – ICAE2014

Promising Surface Modification Strategies for High Power Conversion Efficiency Dye Sensitized Solar Cell Based on ZnO Composite Photoanode

Yu-Tung Yin and Liang-Yih Chen*

Department of Chemical Engineering, National Taiwan University of Science and Technology, 43, Section 4, Keelung Road, Taipei, 106, Taiwan.

Abstract

ZnO nanowires (NWs)/nanoparticles (NPs) composites grown on the indium-doped tin oxide (ITO) substrates by were used as photoanodes of dye-sensitized solar cells (DSSCs). Well-aligned ZnO NWs were synthesized by continuous flow injection (CFI) system. To increase dye absorption area, ZnO NPs were subsequently decorated on the surfaces of ZnO NWs via base-free chemical bath deposition (CBD). According to analysis of electrochemical impedance spectroscopy (EIS), the electron diffusion coefficient (D_n) inside the ZnO NWs/NPs photoanode was 3.9×10^{-3} cm^2/s, which indicated high electron transport properties in this work. The conversion efficiency of DSSCs via D149 sensitized ZnO composite photoanode could achieve 5.24%. To furthermore increase the conversion efficiency, the surface modification process was necessary. In this study, 4-tert-butylpyridine (4-*t*BP) and water vapor was employed on the ZnO composite photoanodes. After treatment by 4-*t*BP, water molecules and applied both processes on the surfaces of ZnO NWs/NPs photoanodes, the conversion efficiencies of DSSCs could be improved from 5.25% to 5.71%, 6.30% and 6.60%, respectively. The possible enhancement mechanism could be conducted by EIS technique in this work.

Peer-review under responsibility of the Organizing Committee of ICAE2014

Keywords: D149, dye-sensitized solar cells, DSSC, electron transport, surface treatment, 4-*t*BP

Introduction

Since the convenient production process, low materials cost, and over 12% efficiency, dye-sensitized solar cells (DSSCs) has become a promising photovoltaic device in the future [1]. However, a multiple trapping/de-trapping electron diffusion process occurs in conventional nanoparticles (NPs) based DSSC, which results in slow electron transport properties. Owing to above behaviors, electrons would lost by

* Corresponding author. Tel.: +886-2-2737-6615; fax: +886-2-2737-6644.
E-mail address: Sampras@mail.ntust.edu.tw

Peer-review under responsibility of the Organizing Committee of ICAE2014
doi:10.1016/j.egypro.2014.12.071

recombination with oxidizing agents in electrolyte and oxidized dyes on the surfaces of photoanodes [2]. The superior electron transport properties have already been demonstrated in nanowires (NWs) based DSSCs by using well-aligned and single crystalline ZnO NWs [3].

In this work, 4-*tert*-butylpyridine (4-*t*BP) and water molecules were used for the first time to modify the surfaces of ZnO-based photoanodes. A controlled ZnO NPs/NWs DSSCs without any surface treatment had an average efficiency of 5.24%. After reducing multilayer dye absorption and electron-hole recombination loss by 4-*t*BP and water molecules, the efficiencies were improved to arrive 5.71% and 6.30%, respectively. At last, we also applied both surface treatments to optimum the dye absorption situation of the ZnO NPs/NWs photoanodes, the efficiency of ZnO-based DSSCs could achieve 6.59%.

2. Experimental section

Well-aligned ZnO NW arrays were first grown on the seeded ITO substrates by CFI process, which has been described elsewhere [4]. The epitaxial growth of ZnO NPs were constructed by CBD process with a methanolic solution of 0.15 M zinc acetate ($ZnAc•2H_2O$, Sigma-Aldrich, 99.5%). The morphologies and structural characterizations of the as-synthesized photoanodes were examined by electron microscope (SEM, JEOL JSM-6500F) and transmission electron microscope (TEM, Philips Tecnai F20 G2), respectively. For DSSCs, D149 dye (Mitsubishi Paper Mills Ltd) was used as sensitizer in this work. The surface treatments would be conducted by immersing ZnO NPs/NWs photoanodes in 3 mL of 4-*t*BP solution in room-temperature and water vapor in ambient, respectively. After treatment, the photoanode would be sandwiched sealed with a platinized fluorine-doped tin oxide (FTO) substrate by 50 μm hot-melt spacers (SX 1170-25×2, Solaronix SA). Liquid electrolyte solution, which composed of 0.5 M of Pr_4NI (ACROS, 99.5%) and 50 mM of I_2 (Sigma, 99.8%) in 4:1 volume ratio of acetonitrile and ethylene carbonate, was injected between two electrodes via a pre-drilled hole.

The photovoltaic performances of the DSSCs were characterized under AM 1.5 solar simulator with 100 mW/cm^2 (150 W, Model 92250A, Oriel). A power source meter (Keithley 2400) was used to record the response of DSSCs. Electrochemical impedance spectroscopy (EIS) was conducted by using a potentiostate (AUTOLAB PGSTAT 302N) with frequency response analyzer (FRA) module operating in two electrode configuration. Measurements have been carried under various biases with 50 mV amplitude and frequency domain from 0.5 Hz to 100 kHz under in illumination and dark environment, respectively.

3. Results and Discussion

The as-grown ZnO NWs and ZnO NPs/NWs photoanodes were shown in Fig. 1(a)-(b). For ZnO NPs/NWs photoanodes, ZnO NPs were epitaxial grown on ZnO NWs via base-free CBD process without any structure directing agents. Microstructures of the ZnO NPs/NWs photoanodes were carried out by transmission electron microscopy (TEM). The dark field image under [0002] zone axis and high-resolution TEM images indicated the epitaxial relationship between ZnO NWs and NPs, as shown in Fig. 1(c)-(d). The epitaxial growth for ZnO NPs provided a convenient path for electron transport.

In the following, ZnO NPs/NWs arrays with various surface treatments were applied before DSSCs assembling for discussion. We labeled them as (a) non-treated, (b) 4-*t*BP treated, (c) water vapor treated and (d) both 4-*t*BP and water vapor treated ZnO NPs/NWs photoanodes. The performances of incident photocurrent conversion efficiency (IPCE) and current density-voltage (J-V) curves were shown in Fig. 2 (a)-(b) and the performances of short current density (J_{sc}), open-circuit voltage (V_{oc}), filling factor (FF) and conversion efficiency (η) of surface treated ZnO NPs/NWs DSSCs were listed in Table 1. According

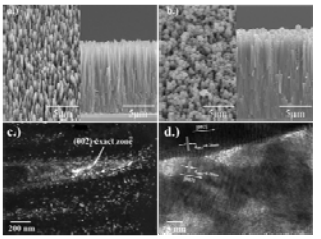

Fig. 1. SEM images photoanodes of (a) ZnO NWs; (b) ZnO NPs/NWs. The corresponding of (c) dark-field image and (c) high resolution images of ZnO NPs/NWs

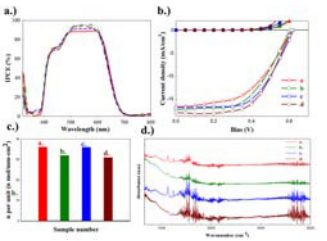

Fig. 2. (a) IPCE; (b) J-V curves; (c) dye loading amounts and (d) FT-IR spectra of four different kinds of ZnO-based photoanodes.

to efficiency analysis, the controlled ZnO NPs/NWs photoanode without any surface treatment has η of 5.25%. After 4-*t*BP treatment, J_{sc} and η increased to 17.38 mA/cm^2 and 5.71%, respectively. When ZnO NPs/NWs photoanode was treated by water vapor, the J_{sc} with similar value, but FF and η increased to 0.60 and 6.30%, respectively. When ZnO NPs/NWs photoanode treated by 4-*t*BP and water vapor sequentially, J_{sc}, FF and η of DSSCs increased to 17.97 mA/cm^2, 0.60 and 6.59%, respectively.

To figure out the possible enhancement mechanism, dye loading amounts were analyzed by UV-visible absorption spectra, as shown in Fig. 2(c). For 4-*t*BP treatment, the dye loading amount decreased after treatment; however, the similar amount for water vapor treated photoanode. We also used Fourier-transfer infrared (FT-IR) spectroscopy to identify the anchoring group in these treated photoanodes, as shown in Fig. 2 (d). The photoanode treated by 4-*t*BP could not observe specific peaks of 4-*t*BP molecules. However, there were obvious peaks of hydroxyl group, which stand for H_2O molecules around 1400-1600cm^{-1} and 3600-3900cm^{-1} for water vapor treated photoanodes.

Electrochemical impedance spectroscopy (EIS) analysis was also carried to examine the electron transport properties in ZnO NPs/NWs photoanodes with various surface treatments. A typical EIS response could be taken under 1 sun (100 mW/cm^2) illumination and in the dark environment. In Fig. 3 (a), the charge transport resistance (R_t), charge transfer resistance (R_{ct}), chemical capacitance (C_μ), transient time (τ_d), recombination lifetime (τ_n) and effectively diffusion length (L_n) of various surface treated ZnO NPs/NWs DSSCs were analyzed by EIS biased at V_{oc} under 1 sun illumination. To determine the parameters of electron transport inside ZnO NPs/NWs photoanode, an equivalent circuit model, as shown in Fig. 3(b), was employed and the fitting parameters were listed in Table 2. From EIS analysis under 1 sun illumination, we could find the transient time of 4-*t*BP treated ZnO NPs/NWs DSSCs slightly reduced and that of water vapor treated ZnO NPs/NWs DSSCs significantly reduced to 0.23 ms. Comparing with controlled ZnO NPs/NWs photoanode (sample a), R_t and R_{ct} were similar for four samples. However, the values of C_μ were different for four surface treated ZnO NPs/NWs photoanodes.

Table 1. Performances of DSSCs with various surface treatments.

Sample ID	Photoanodes	J_{sc} (mA/cm^2)	V_{oc} (V)	FF	η (%)
a	Non-treated	16.71	0.61	0.51	5.25
b	4-*t*BP treated	17.38	0.61	0.54	5.71
c	H_2O treated	16.88	0.62	0.60	6.30
d	4-*t*BP/H_2O treated	17.97	0.61	0.60	6.59

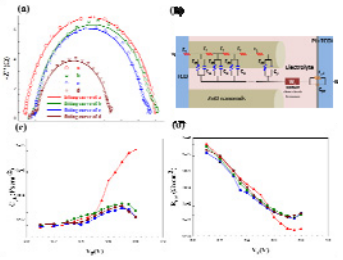

Fig. 3. (a) EIS analysis under 1 sun illumination; (b) the corresponding equivalent circuit model; (c) C_μ vs. V and (d) R_{ct} vs. V for four different surface treated ZnO NPs/NWs photoanodes.

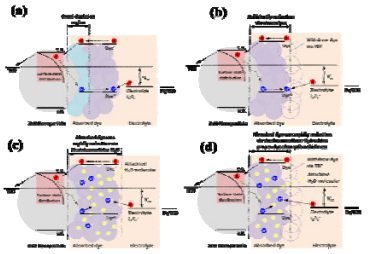

Fig. 4. Schematic diagram of electron transport in four different ZnO NPs/NWs photoanodes. (a) controlled; (b) 4-*t*BP treated; (c) water vapor treated and (d) both 4-*t*BP and water vapor treated.

To understand the detail transport properties for the influence of surface treatment ZnO NPs/NWs photoanodes, EIS was analyzed in the dark with various biases of 0.1V to 0.8 V, as shown in Fig. 3(c)-(d). The varieties of C_μ and R_{ct} of controlled ZnO NPs/NWs photoanode under various biases were different to that of surface treated ZnO NPs/NWs photoanodes. The electron accumulation in the controlled ZnO NPs/NWs photoanode was obviously. After 4-*t*BP and water vapor treatment, the electron accumulation can be improved due to low C_μ. Combining dye loading amount, FT-IR and EIS analyses, we proposed a scheme of electron transport of a high power conversion efficiency of ZnO NPs/NWs DSSCs after surface treatment, as shown in Fig. 4.

Table 2. EIS fitting parameters for various surface treatments under illuminated condition.

Sample No.	Photoanode	R_t (Ω)	R_{ct} (Ω)	C_μ (μF)	τ_n (ms)	D_n (cm^2/s)	τ_d (ms)	L_n (μm)
a.	Non-treated	0.99	15.07	448.84	6.77	3.94×10^{-3}	0.45	51.64
b.	4-*t*BP treated	0.99	13.39	334.31	4.48	5.29×10^{-3}	0.34	48.68
c.	H_2O treated	0.99	12.68	239.08	3.03	7.40×10^{-3}	0.23	47.37
d.	4-*t*BP/H_2O treated	0.95	8.47	275.66	2.34	6.64×10^{-3}	0.26	39.37

4. References

[1] Yella A, Lee HW, Tsao HN, Yi C, Chandiran AK, Nazeeruddin MK, Diau EWG, Yeh CY, Zakeeruddin SM, Grätzel M, Porphyrin-sensitized solar cells with cobalt (II/III)–based redox electrolyte exceed 12 percent efficiency. *Science* 2011;**334**: 629-34.

[2] Kang SH, Choi SH, Kang MS, Kim JY, Kim HS, Hyeon T, Sung YE, Nanorod-based dye-sensitized solar cells with improved charge collection efficiency. *Advanced Materials* 2008;**20**:54-8.

[3] Wong DKP, Ku CH, Chen YR, Chen GR,Wu JJ, Enhancing electron collection efficiency and effective diffusion length in dye-sensitized solar cells. *ChemPhysChem* 2009;**10**:2698-702.

[4] Chen LY,Yin YT, Facile continuous flow injection process for high quality long ZnO nanowire arrays synthesis. *Crystal Growth & Design* 2012;**12**:1055-9.

Biography

Liang-Yih Chen is currently Associated Professor of the Department of Chemical Engineering, National Taiwan University of Science and Technology (NTUST, Taiwan-Tech). His current research interests include the synthesis of semiconductor quantum dots, one-dimensional metal oxide nanomaterial synthesis and sensitized solar cells. *Yin Yu-Tung* now joined the doctoral program under the supervision of Prof. Liang-Yih Chen from 2008. His research focused on the growth of 1D nanostructures, developed the solar cells devices and the studies of transport phenomena of electrons of dye-sensitized solar cells by using electrochemical impedance spectroscopy technique.